

Synthesis and Applications of  
 $\pi$ -Extended Naphthalene DiimidesCheng Li,<sup>[a]</sup> Zhi Lin,<sup>[a,b]</sup> Yan Li,<sup>\*,[a]</sup> and Zhaohui Wang<sup>[a]</sup>

**ABSTRACT:** Naphthalene diimides have received much attention due to their high electron affinities, high electron mobility, and good thermal and oxidative stability, therefore making them promising candidates for a variety of organic electronic applications. However,  $\pi$ -extended naphthalene diimides with lower HOMO-LUMO gaps and higher stability have only been developed recently because of the synthetic difficulties. This account describes recent developments in the structures, synthesis, properties, and applications of  $\pi$ -extended naphthalene diimides, including pure-carbon and heterocyclic acene diimides, from our research group.

**Keywords:** acene diimides, heterocycles, naphthalene diimides, organic field-effect transistors, semiconductors

## 1. Introduction

Organic semiconductors, as low-cost, flexible, lightweight, and printable materials, have been of great research interest for use as key components in next-generation optoelectronic devices, such as organic field-effect transistors (OFETs) and organic photovoltaic devices (OPVs).<sup>[1]</sup> At present, many p-channel conjugated polycyclic aromatic hydrocarbons (PAHs), such as oligoacenes and oligothiophenes, have achieved delightful device performance,<sup>[2]</sup> while n-channel organic semiconductors are less numerous and the device performance leaves much to be desired. Recently, aromatic diimides, particularly naphthalene diimides

(NDIs) and perylene diimides (PDIs), have received much attention for their high electron affinities, high electron mobility, and excellent thermal stability.<sup>[3]</sup> At present, aromatic diimides are promising candidates as n-channel organic semiconductors for a variety of organic electronic devices. Several overviews have already been written, but this area develops very fast.<sup>[3,4]</sup>

Structurally, aromatic diimides are composed of an aromatic core and two electron-withdrawing imide groups. Typically, the core functionalization can dramatically alter the optical and electrochemical properties, even with relatively small structural changes at the aromatic core. The nitrogen atoms of imide groups can be further modified by a variety of alkyl or aryl substituents, on the contrary, which normally have little effect on the optical and electrochemical properties, but have a significant influence on the solubility, crystallinity, and aggregation behavior. According to the aromatic core, aromatic diimides can be divided into acene diimides and rylene diimides.

## 1.1. Acene Diimides

Acene diimides, composed of an acene core and two imide groups, can be broadly split into two basic types, based on the imide rings – the five-membered imide ring type and the six-membered imide ring type, as shown in Figure 1. The five-membered imide ring type (Figure 1, **1**) is usually synthesized via the Diels-Alder aromatization reaction by maleimide and

<sup>[a]</sup>C. Li, Z. Lin, Y. Li, Z. Wang  
Beijing National Laboratory for Molecular Sciences,  
Key Laboratory of Organic Solids,  
Institute of Chemistry  
Chinese Academy of Sciences  
Beijing 100190  
(P. R. China)  
E-mail: yanli@iccas.ac.cn

<sup>[b]</sup>Z. Lin  
College of Chemistry and Molecular Engineering  
Peking University  
Beijing 100871  
(P. R. China)

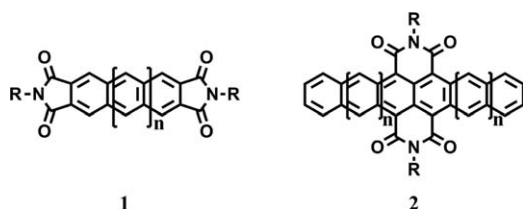


Fig. 1. Two types of acene diimides.

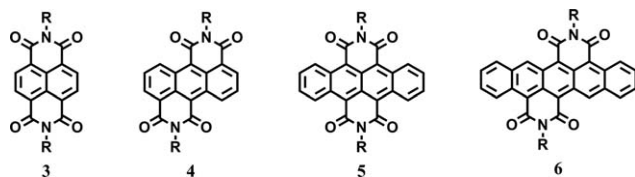


Fig. 2. Selected examples of acene diimides: naphthalene diimides (3); anthracene diimides (4); tetracene diimides (5); pentacene diimides (6).

the corresponding acene derivatives.<sup>[5]</sup> It is known that the introduction of electron-withdrawing groups at the *peri*-positions of acenes can change the electronic and optical properties drastically. So our research group focuses on the six-membered imide ring acene diimides (Figure 1, 2), which can be derived from both the NDI scaffold by ring extension and the amidation of acenes. So far, only a few kinds of these acene diimides have been reported due to the synthetic difficulties. In 2011, Wudl synthesized the anthracene diimides (Figure 2, 4).<sup>[6]</sup> Yamada and coworkers established a unique bismuth triflate-mediated double-cyclization approach to obtain anthracene diimides (Figure 2, 4), tetracene diimides (Figure 2, 5), and penta-

cene diimides (Figure 2, 6).<sup>[7]</sup> At almost the same time, our group reported the facile synthesis of tetracene diimide.<sup>[8]</sup> Until recently, the synthesis of symmetric larger PAH diimides with multi-imides at the *peri*-positions of the aromatic core had only been achieved by our group.<sup>[9]</sup> The synthesis of high acene diimides is still a difficult and challenging task, owing to the lack of effective synthesis strategies. Therefore, it is a very urgent issue to develop new synthesis strategies for larger acene diimide derivatives for the further study of their structure-property relationships and applications.

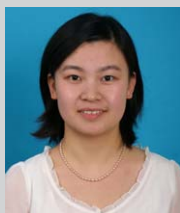
## 1.2. Heterocyclic Acene Diimides

Heterocyclic acene diimides can be considered as the product of exchanging CH units of acene diimides with heteroatoms such as nitrogen and sulfur. The past five years have witnessed the explosive growth of studies on the synthesis, properties, and applications of larger heterocyclic acene diimides. In 2010, Gao and coworkers developed a series of malonitrile-based NDI derivatives which exhibited outstanding air-stable n-type semiconducting properties (Figure 3, 7).<sup>[10]</sup> Meanwhile, they also demonstrated a systematic study on the relationship between film microstructure and charge transport in their organic thin-film transistors by four NDI derivatives with different lengths and branching-point alkyl chains.<sup>[11]</sup> In 2011, a core-extended NDI, fused with highly electron-rich carbazole rings, was synthesized by Würthner and coworkers, and it proved to be an ambipolar semiconductor (Figure 3, 8).<sup>[12]</sup> In 2012, Zhao reported the characterization of quinonoid tautomers of dihydrotetraazaacene derivatives.<sup>[13]</sup> Based on this, they also

Cheng Li received his B.Sc. degree at the department of chemistry, Beijing Normal University in 2010, and his Ph.D. in 2015 from the Institute of Chemistry, Chinese Academy of Sciences, under the supervision of Prof. Zhaohui Wang. Since then, he has been working at this institute as an assistant professor. His research interests include the design, synthesis, and application of organic semiconducting materials.



Yan Li received her B.S. degree (2005) at the School of Petrochemical Engineering, Changzhou University, and her M.S. degree (2008) at the China University of Mining and Technology. She then joined the Institute of Chemistry, Chinese Academy of Sciences (CAS), and received her Ph.D. degree in 2012, under the supervision of Prof. Zhaohui Wang. Now, she is working at this institute as an associate professor. Her research interests include the design and syn-



thesis of organic functional molecules and their device applications.

Zhaohui Wang received his B.S. degree in 1990 at the Department of Chemical Engineering, Nanjing University of Science and Technology, and M.S. degree in 1995 and Ph.D. degree in 1999 from the East China University of Science and Technology. From 1999 to 2005, he stayed at the MaxPlanck Institute for Polymer Research in Mainz as a research scientist. In 2005, he joined the Key Laboratory of Organic Solids, Institute of Chemistry, Chinese Academy of Sciences as a professor. His research interests relate to functional conjugated molecules and molecular devices.



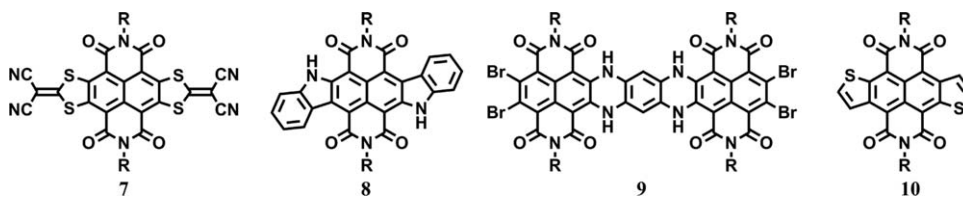


**Fig. 3.** Selected examples of heterocyclic acene diimides: malonitrile-fused NDI (7); carbazole-fused NDIs (8); hydroazaheptacene tetraimides rylene diimides (9); and thiophene-fused NDIs (10).

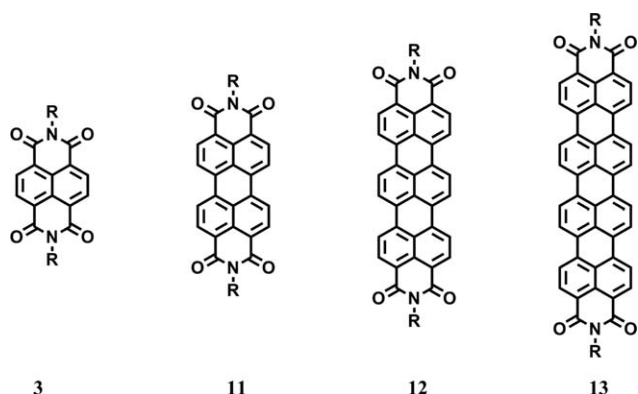
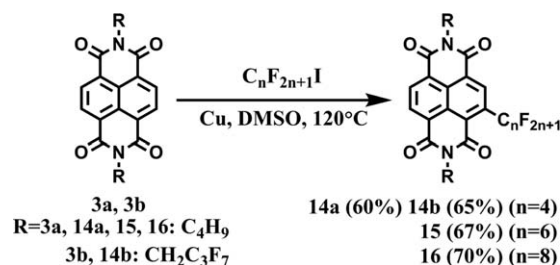


**Fig. 4.** Selected examples of rylene diimides: naphthalene diimides (3); perylene diimides (11); terrylene diimides (12); and quaterrylene diimides (13).

synthesized some hydroazaacene dicarboximide derivatives as useful NIR materials, in 2014 (Figure 3, 9).<sup>[14]</sup> In addition, Takimiya established a reliable and straightforward access to  $\alpha,\beta$ -unsubstituted and  $\alpha$ -halogenated thiophene-fused NDIs in 2013 (Figure 3, 10).<sup>[15]</sup> Heterocyclic acene diimides are relatively more readily available than acene diimides. This is because the synthesis of acene diimides often involves the formation of numerous complex carbon-carbon bonds and ring extensions, while the synthesis of heterocyclic acene diimides regularly allows the use of simpler synthetic strategies, even just some easily accessed nucleophile substitutions, such as simple condensations of 1,2-phenylenediamines with 1,2-dibromides. Moreover, the introduction of heteroatoms to the  $\pi$ -skeleton of acene diimides offers several important advantages, since the resulting heterocyclic acene diimides are easy to dissolve and less susceptible to degradation through oxidation. Besides, the electronic structures and molecular packing of those heterocyclic acene diimides can be flexibly controlled by the number, position, and valence state of heteroatoms within the  $\pi$ -skeleton. Consequently, we are continually working to develop new methods to afford larger heterocyclic acene diimides.

### 1.3. Rylene Diimides

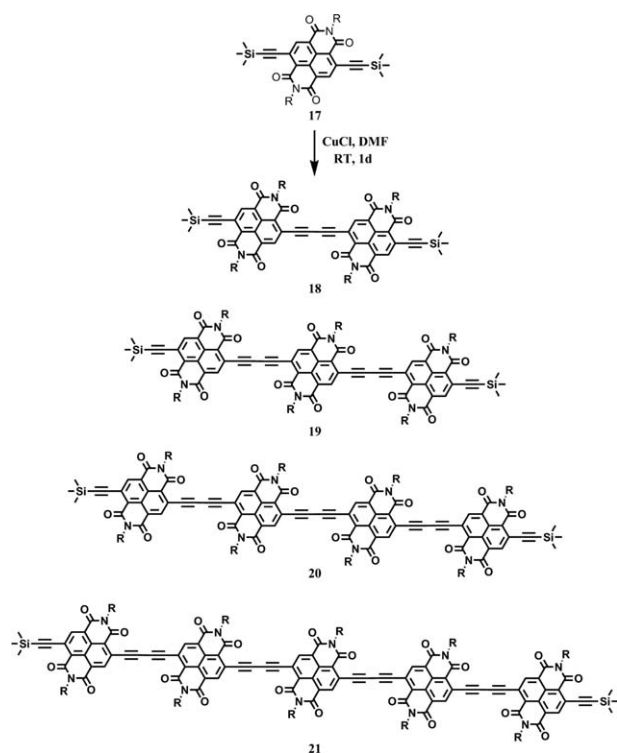
Rylene diimides, made up of naphthalene units linked in *peri*-positions, has been fascinating a crowd of scientists for decades



**Scheme 1.** Perfluoroalkylation of NDIs.

because of their perfect graphene ribbon-like structures and outstanding electronic and optical properties. Figure 4 shows selected examples of rylene diimides, among which, NDIs and PDIs are considered as the most representative and promising rylene diimides, which have already achieved excellent electron-transport performance and could even compete with their p-channel counterparts, owing to their low-lying LUMO levels and highly reversible redox behavior.<sup>[16]</sup> As the extension of the aromatic  $\pi$ -system along the molecular long axis of rylene diimides, the absorption has become progressively red-shifted to the near-infrared region (NIR), and the absorption coefficients have simultaneously increased.<sup>[17]</sup> But the synthesis to obtain these higher rylene diimides usually involves a complex multistep reaction approach, which leads to a relatively low overall yield. So, despite all the achievements in the chemical modification of rylene diimides, exploring effective synthesis strategies for expansion into the construction of homologous series of rylene diimides still remains an arduous challenge in organic and materials chemistry. In recent years, our research group has achieved much in the design and synthesis of laterally expanded aromatic diimides based on the homo-coupling and cross-coupling reactions of core-functionalized NDIs and PDIs, as well as their preliminary applications, both in OFETs and OPVs.<sup>[18]</sup>

Above all, the design, synthesis, and characterization of new aromatic diimides are basic aspects for the development of next-generation optoelectronic devices. NDIs, the smallest homologue of rylene diimides and also the smallest homologue of acene diimides, are considered the most promising building blocks to construct ideal semiconducting materials. In this account, we will describe the chemistry of  $\pi$ -extended NDIs,



**Scheme 2.** One-pot synthesis of oligo-butadiynylene-NDIs.

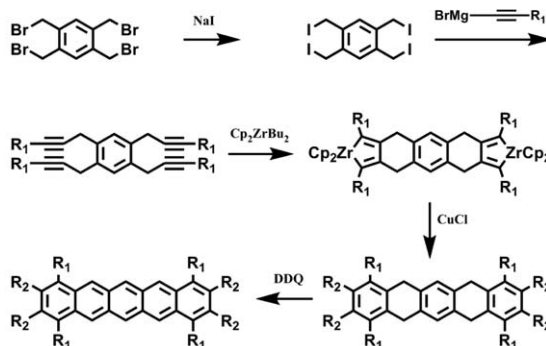
including acene-type diimides and heterocyclic acene-type diimides investigated by our research group since 2010. Through this research, many efficient methods for the synthesis of laterally expanded NDIs have been established. Most of the resulting acene diimides and heterocyclic acene diimides have narrow HOMO-LUMO gaps, strong light-absorbing abilities and excellent electron-transport properties. Some preliminary results of the applications of partial acene diimides and heterocyclic acene diimides in OFETs are also described.

## 2. Synthesis Strategies for $\pi$ -Extended Naphthalene Diimides

### 2.1. Core Functionalization of NDIs through C–H Bond Activation

As early as 2010, our group began research on core functionalization of NDIs. Incorporating strong electron-withdrawing groups, such as the cyano group, fluorine atoms, and fluoroalkyls, into the aromatic core is one of the key design principles for air-stable n-type semiconductor materials. Some PDI and NDI derivatives with cyano and fluoroalkyl groups have been reported as air stable n-type semiconductors with high mobilities.<sup>[19]</sup> Meanwhile, in the past several decades, the continued development of transition-metal-mediated direct C–H functionalization/C–C bond formation methods has provided

### Takahashi's Double Homologation Method



### Shimizu's Double Cross-Coupling Method

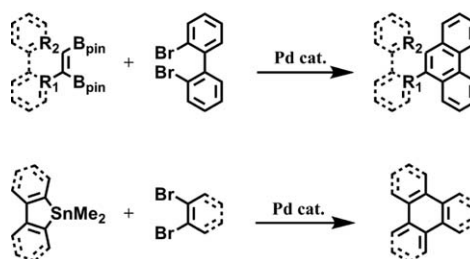
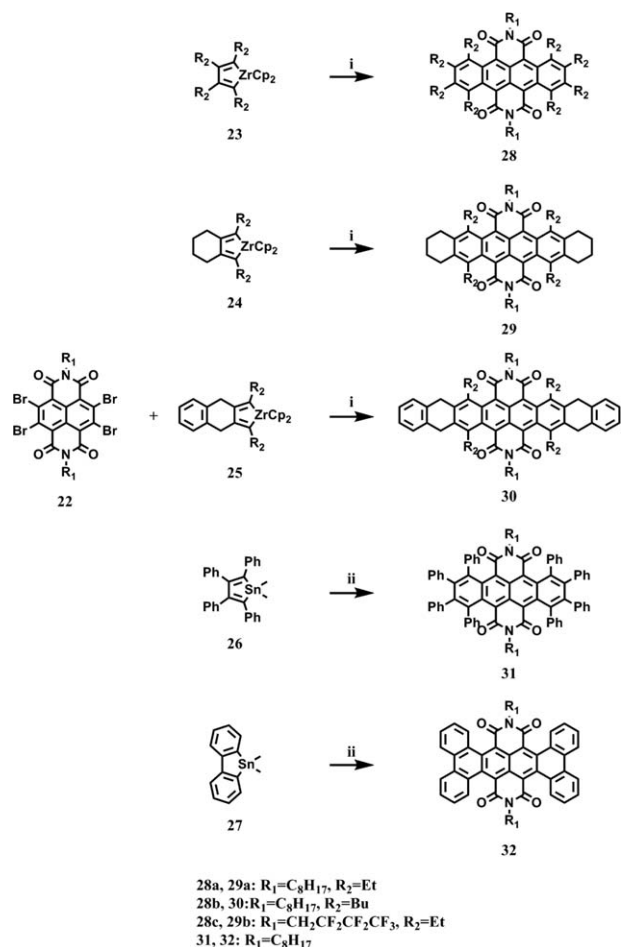


**Fig. 5.** Double cross-coupling strategies for ring expansion.

many more opportunities to implement novel synthetic strategies. So one of our ideas was direct perfluoroalkylation of NDIs by C–H bond activation.

On our first few attempts, the direct functionalization of the electron-deficient NDI core via copper-mediated radical perfluoroalkylation was achieved.<sup>[20]</sup> As shown in Scheme 1, the direct perfluoroalkylation of the NDI core gave mono-perfluoroalkylated NDIs with excellent yields. The effect of the perfluoroalkyl length on yield was not obvious. However, there was no desired product detected while using bromo-NDIs as reactants under the same conditions, which was different from the perfluoroalkylation of bromo-PDIs. This method was also applied to many electron-rich polycyclic aromatics, such as naphthalene, pyrene, and perylene. It should be mentioned that the perfluoroalkyl chain was regioselectively introduced to the 1-position of naphthalene and pyrene, and the 3-position of perylene. The absorption spectra, emission spectra, and cyclic voltammograms of those core-functionalized NDIs did not vary greatly with the perfluoroalkyl length. But compared with their parents, **3a** and **3b**, the maximum absorption spectra of the perfluoroalkylated NDIs (**14a** and **14b**) red-shifted by 4 nm. Both **14a** and **14b** obtained higher first and second reduction waves, indicating that core perfluoroalkylation could lower the LUMO levels. As for **15** and **16**, the length of the fluorinated alkyl chain has little influence on the absorption, emission spectra, and cyclic voltammograms. We





**Scheme 3.** The synthetic route of tetracene diimides by double cross-coupling strategies. conditions: i) Zirconacyclopentadiene, CuCl, THF, 50°C, argon; ii) Pd(P(*t*-Bu)<sub>3</sub>)<sub>2</sub>, CsF, THF, 70°C, argon.

also confirmed the radical mechanism of this method by adding radical scavengers to the reaction mixture.

## 2.2. Core Functionalization of NDIs through Metal-catalyzed Coupling Reactions

Over the past 30 years, the development of a wide variety of new metal-catalyzed cross-coupling reactions have profoundly changed the protocols for the construction of organic compounds and led to the construction of materials in organic electronics from simpler entities. Therefore, we are particularly interested in the design and synthesis of novel  $\pi$ -extended NDIs through metal-catalyzed coupling reactions.

We supposed that combining multi-NDI moieties into one molecule might be another design principle for air-stable n-type semiconductor materials, but the traditional stepwise approaches for the synthesis of oligomers often required long and repetitious processes with low overall yields. Therefore, our strategy was developing new approaches to get core-

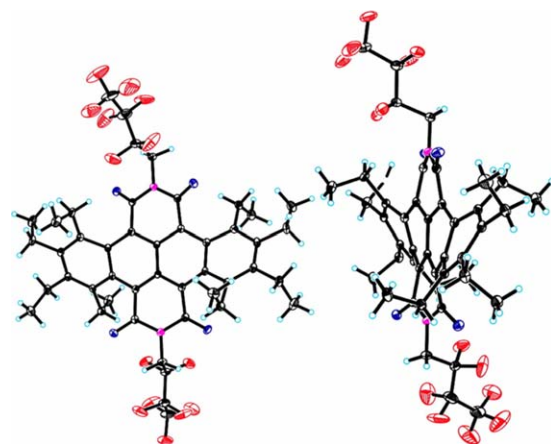


**Fig. 6.** X-ray crystallographic structures of 28c.

functionalized NDI oligomers just by one-pot reactions. Later, we reported the successful synthesis of well-defined oligo-butadiynylene-NDIs by a one-pot reaction under extremely mild conditions.<sup>[21]</sup> As shown in Scheme 2, a series of soluble linearly conjugated NDI oligomers containing multi-NDI moieties were directly obtained by the homocoupling of 2,6-di((trimethylsilyl)ethynyl)-NDI **17** in the presence of a stoichiometric amount of CuCl in DMF at room temperature. Although we got at least four products – up to five NDI moieties in just one reaction – the yields were acceptable: **18** (32%), **19** (25%), **20** (16%), and **21** (7%). The maximum absorption wavelength of these homogeneous oligomers with different length units in solution became progressively red-shifted (**18**: 482 nm; **19**: 498 nm; **20**: 506 nm; and **21**: 510 nm) and the molar absorption coefficient almost increased linearly with the increasing number of NDI units, as a reflection of the extended conjugation length of the NDI core. It was interesting that the extent of the redshifts from compounds **18** to **21** (44 nm, 16 nm, 8 nm, and 4 nm) were not linear, probably due to the effective conjugation length approaching saturation.

As mentioned in the introduction, only a very limited number of methods for the synthesis of tetracene diimides have been reported since 2010. Yamada described the first synthesis of tetracene diimides via bismuth triflate-mediated double-cyclization reaction of acid chlorides and isocyanates in 2010.<sup>[7]</sup> Chi also reported the synthesis of tetracene diimides by a FeCl<sub>3</sub>-mediated oxidative cyclodehydrogenation reaction in the next year.<sup>[22]</sup> Although many groups have been working on the synthesis of tetracene diimides and have made a lot of contributions, it remains a tough task to efficiently synthesize these well-defined tetracene diimides for organic semiconductor materials.

Structurally, acene diimides can be derived from the NDI scaffold by the extension of more benzene rings. Thus, our

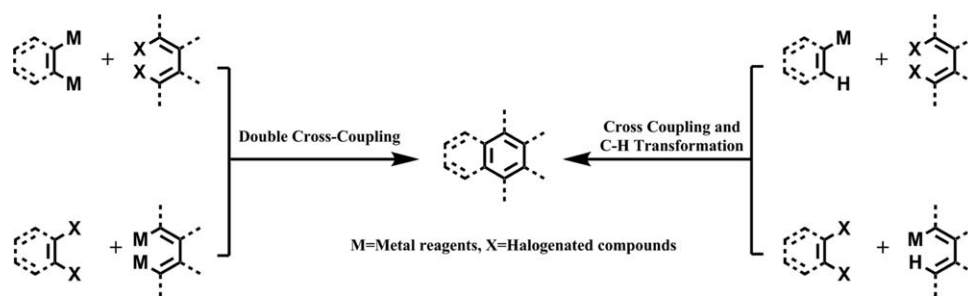


Fig. 7. Comparison of double cross-coupling and cross-coupling/C–H transformation strategies.

strategy to create new series of acene diimides as n-type organic semiconductor materials is to explore novel ring-expansion reactions using the NDI scaffold as preliminary building block. Over the past few years, the transition-metal-catalyzed double cross-coupling reaction of organodimetallic reagents and dihalides has provided an efficient method for the ring extension of PAHs. For example, Takahashi developed a zirconacyclopentadiene-involved double homologation method to extend the aromatic ring system in two directions by tetrayne cyclization to prepare high acene derivatives, as shown in Figure 5.<sup>[23]</sup> Shimizu reported two kinds of palladium-catalyzed double cross-coupling reactions, which provided a variety of triply annulated benzene derivatives in good to excellent yields, also shown in Figure 5.<sup>[24]</sup> However, all those efficient synthetic approaches were used for the synthesis of electron-rich PAHs. The double cross-coupling synthetic approaches based on electron-deficient acene diimides for new functional molecules are rarely reported. So in 2011, we presented the first use of a double cross-coupling synthetic approach for a new family of stable and NIR tetracene diimides in a one-pot reaction under mild conditions, as shown in Scheme 3.<sup>[8]</sup>

As expected, the double cross-coupling of metallacyclopentadiene with electron-deficient NDIs proceeded well to afford the desired tetracene diimides. Specifically, the cross-coupling of compound **22** and zirconacyclopentadiene **23**, **24**, and **25** provided the desired tetracene diimides **28**, **29**, and **30** in the presence of copper chloride in good yield. Similarly, the cross-coupling of compound **22** with 1,1-dimethyl-2,3,4,5-tetraphenylstannole **26** and 9-stannafluorene **27** in the presence of  $\text{Pd}(\text{P}(\text{t-Bu})_3)_2$  gave the corresponding tetracene diimide derivatives **31** and **32**. Due to the extreme steric hindrance of the eight phenyl groups, the yield of compound **31** was moderate. To further achieve higher acene diimides, such as hexacene diimides and octacene diimides, we chose **24** and **25**, which contain cyclohexyl as coupling reagents. Unfortunately, we tried many oxidative dehydroaromatization approaches for compound **29** and **30**, but did not obtain the desired higher acene diimides. Meanwhile, the semiperfluoroalkyl chain, which is known to have a strong influence, not

only on the self-assembled structures of the aromatic core, but also on their transporting properties, was also introduced to the imides position.

The crystal structure of **28c** (Figure 6), obtained by slow evaporation of a solution of dichloromethane and methanol at room temperature, shows that the tetracene core is markedly nonplanar, as well as the two imides rings having dihedral angles of  $30\text{--}32^\circ$  due to the steric encumbrance effect between oxygen atoms and neighboring ethyl groups. All of these new tetracene diimides display broad absorption in solution, covering the whole visible and NIR region from 300 nm to 800 nm, and the maximum absorption wavelength significantly redshifts with higher molar extinction coefficients, when compared with their all-carbon parent, tetracene, owing to the substantial electronic effect of the attachment of strong electron-withdrawing diimides groups at *peri*-positions of the central phenyl rings. Besides, in contrast with the NDI scaffold, tetracene diimides also show much more redshift and smaller band gaps due to the extension of the conjugation by fusing two additional aromatic rings. Moreover, as expected, compound **28c**, with semiperfluoroalkyl chains at the imides position, has a less negative first reduction potential than that of **28a** and **28b**. In view of such unique structures and admirable photophysical and electro-optical properties, this new family of tetracene diimides derivatives is a promising candidate for application in OFETs and OPVs.

### 2.3. Core Functionalization of NDIs through Cross Coupling and C–H Transformations

Encouraged by the success of such facile double-aromatic annulations and the transition-metal-mediated direct C–H functionalization/C–C bond formation methods, we were dedicated to developing novel synthetic strategies: the direct preparation of hybrid rylene imides by the combination of cross coupling and a C–H transformation, as shown in Figure 7. Since NDIs are not stable toward alkylolithiums, we used stannyl NDI derivatives and halogenated PDIs to check the practicability of our concept, envisaging that the Stille-coupling of stannyl NDI with halogenated PDIs would provide a straightforward and promising method for

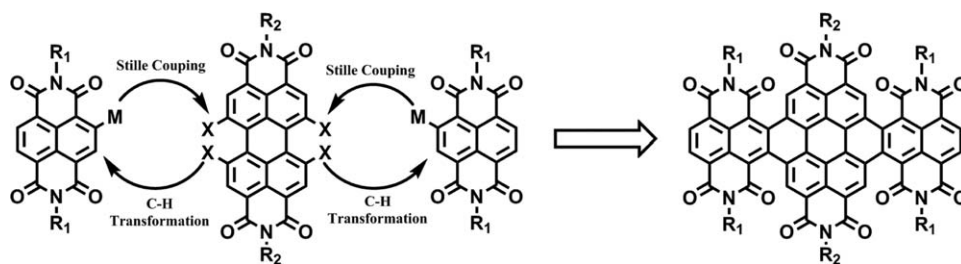
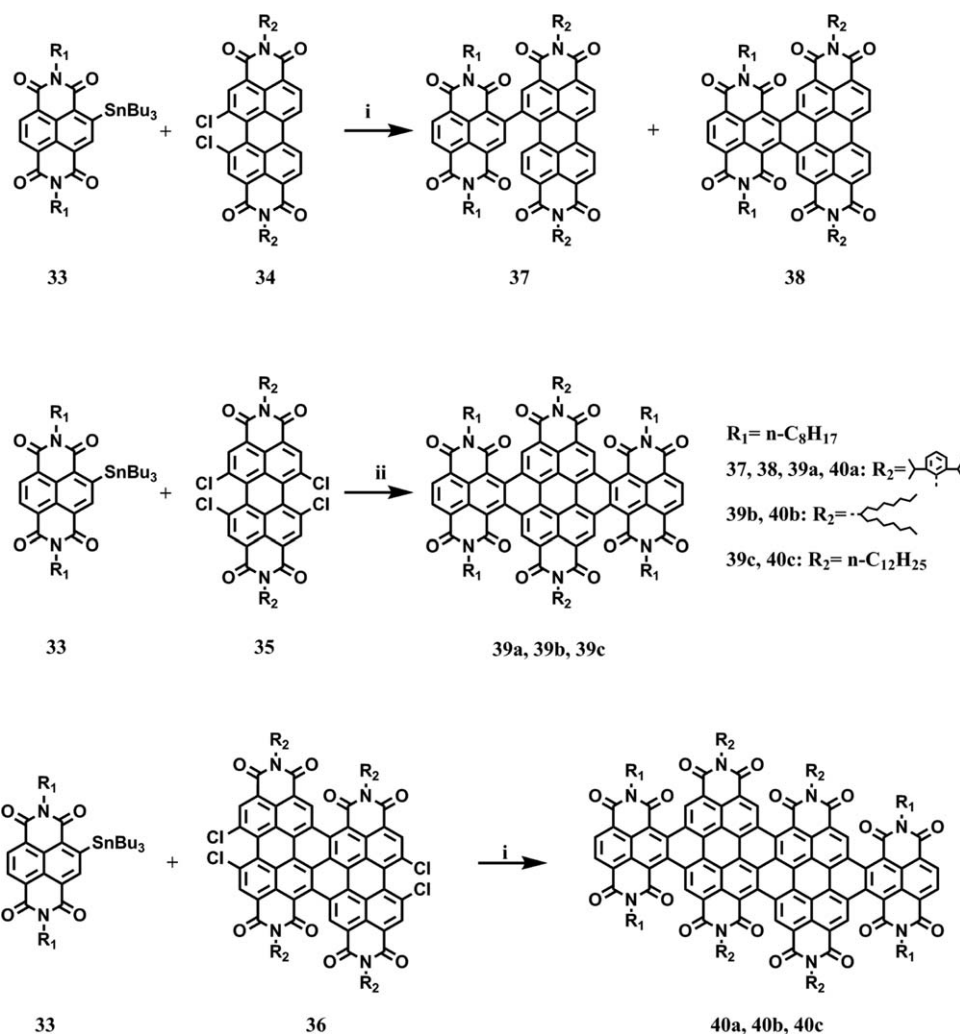


Fig. 8. Synthesis strategy of hybrid NDI-PDI arrays by cross-coupling/C-H transformation.



Scheme 4. Synthesis of hybrid NDI-PDI arrays. Conditions: i)  $\text{Pd}(\text{PPh}_3)_4$ ,  $\text{CuI}$ , toluene, reflux; ii)  $\text{Pd}(\text{PPh}_3)_4$ , toluene, reflux.

construction of fused hybrid NDI-PDI arrays in a one-pot reaction via the cross-coupling/C-H transformation strategy shown in Figure 8.

Fortunately, on our first attempt, the hybrid NDI-PDI arrays **37** and **38** could be successfully achieved in the presence of  $\text{Pd}(\text{PPh}_3)_4/\text{CuI}$  in moderate yield, as shown in Scheme 4.<sup>[9a]</sup>

We found that  $\text{CuI}$  was crucial for the formation of annulated product **38**, and the singly linked NDI-PDI **37** was also afforded as a side product. In addition, different substituents were conveniently introduced into the extended hybrid NDI-PDI-NDI array **39**. The absorption spectrum of **37** is essentially a superposition of those of the NDI and PDI units

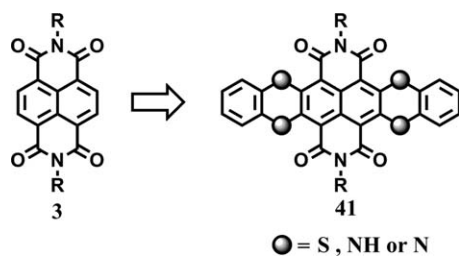


Fig. 9. Chemical structures of six-membered heterocyclic hexacene diimides linked or annulated by heteroatoms.

due to the weak communication between the NDI and PDI. But both **38** and **39** are considerably stronger electron acceptors, which have much less negative first reduction potentials to facilitate electron injection and transport with ambient stability and significantly redshifted absorption, compared with those of the parent NDI and PDI. The OFET performance of compound **39b** was also further investigated.

Inspired by this result, we pursued the further expansion of rylene diimides along the equatorial axis by the fusion of NDI and diPDI units, which led to more broadened absorption and electron affinity, and provided more facilitation of electron transport, as well as stabilization. Fortunately, NDI-diPDI-NDI (Scheme 4, **40**) was obtained by the same facile one-pot synthesis via a combination of Stille coupling and C–H transformation.<sup>[9b]</sup> Such a huge conjugated molecule, possessing eighteen six-membered carbon rings in the core and eight imide groups at the edges, displayed not only broadened and enhanced optical absorptions with the onset absorption wavelength of 736 nm, but also obtained good thermal stability and high electron affinity, with a LUMO level of  $-4.4$  eV. The best OTFT performance was achieved by the linear alkyl chain substituted one, **40c**, with electron mobility as high as  $0.18 \text{ cm}^2 \text{ V}^{-1} \text{ s}^{-1}$  under ambient conditions.

#### 2.4. Core Functionalization of NDIs through Heterocyclization

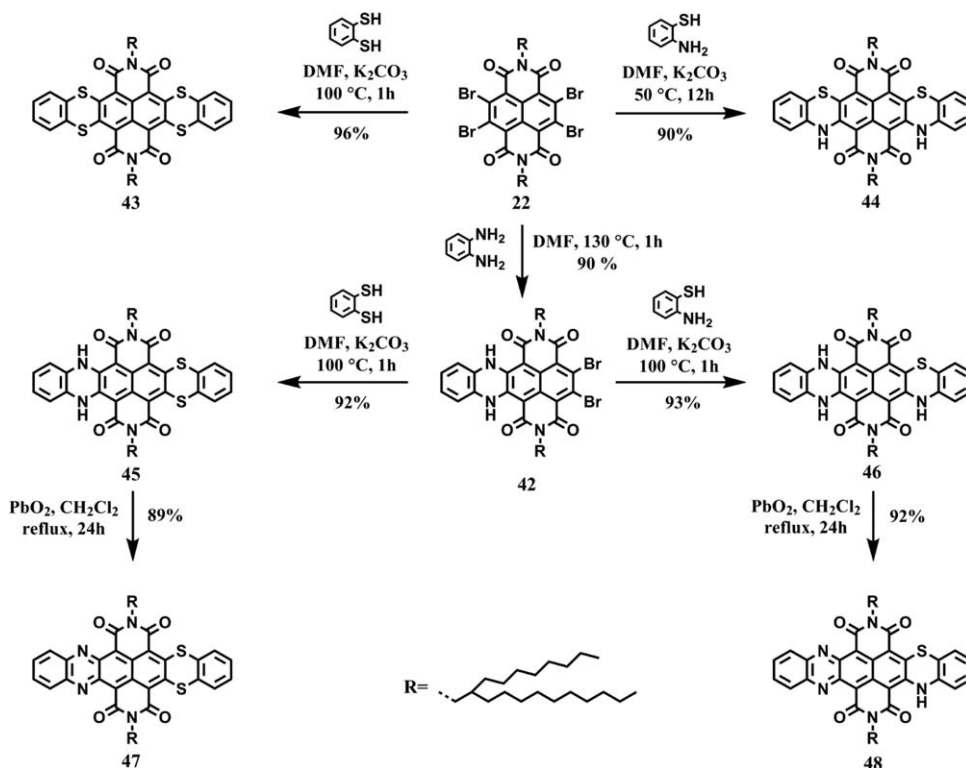
Besides acene diimides based on lateral-extended NDIs with a hydrocarbon aromatic core, we have also paid great attention to heterocyclic acene diimides, due to the unique optical and electrical properties caused by heteroatoms. Before 2013, great progress had been achieved for heterocyclic acene diimides with five-membered heterocycles, both in synthesis and in applications as organic semiconductors. However, the six-membered heterocyclic acene diimides linked or annulated by the mixture of sulfur, nitrogen, and hydronitrogen bridges are rarely reported. On the other hand, in view of the fact that many heteroacenes have also been developed as organic semiconductor materials in organic field effect transistors,<sup>[25]</sup> combining heteroacenes with strong electron-withdrawing imide groups is considered a promising approach for the construc-

tion of new electron-transporting systems. So, at first our thoughts centered on the synthesis, electro-optical properties, and potential applications as organic semiconductors of six-membered heterocyclic acene diimides from the NDI scaffold shown in Figure 9.

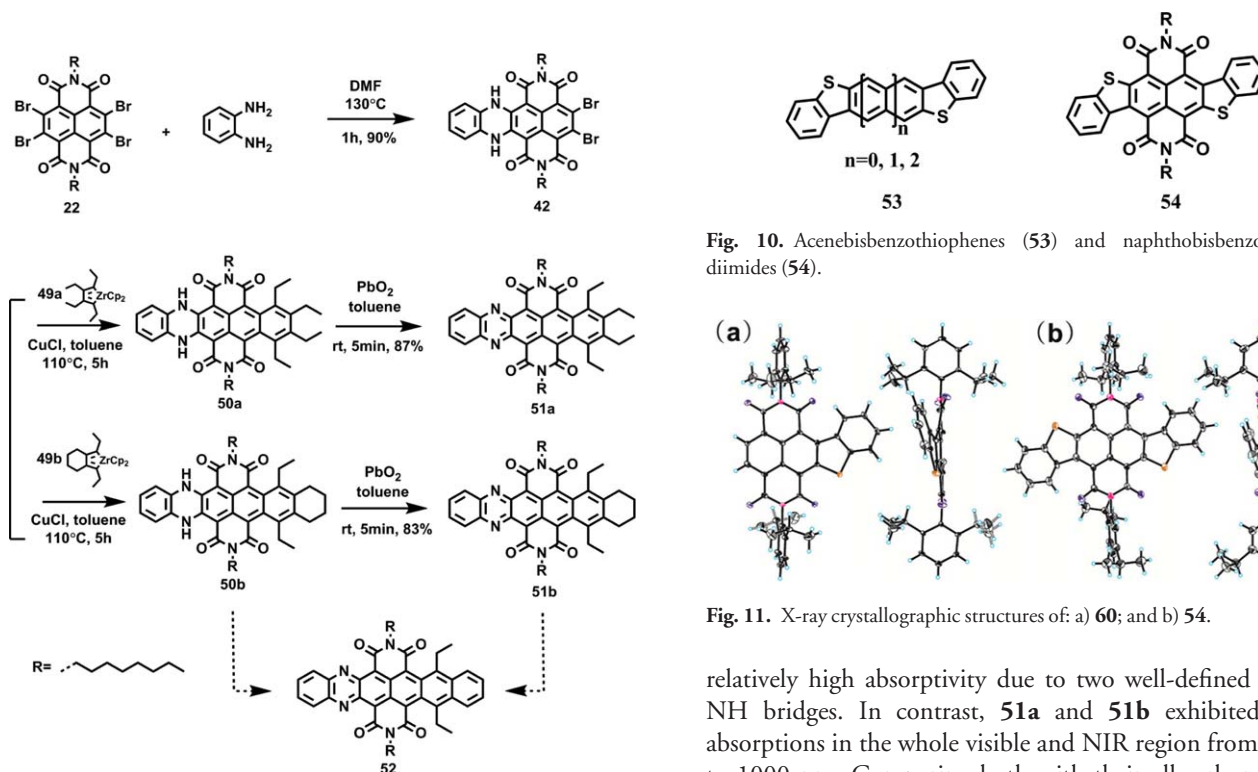
In 2013, we successfully synthesized a series of heterocyclic acene diimides through the condensation of *o*-phenylenediamine, 1,2-benzenedithiol, and 2-aminothiophenol with 4Br-NDI in high yield, as shown in Scheme 5.<sup>[26]</sup> It should be noted that only a one-sided condensed product **42** was obtained, instead of the two-sided one when *o*-phenylenediamine reacted with 4Br-NDI, even with the prolonged reaction time of 2 d. The two remaining bromine atoms of compound **42** are very important for the construction of unsymmetrical heterocyclic acene diimides. It's interesting that the regioisomerically pure compound **44** could be obtained in high yield, which was demonstrated by  $^1\text{H}$  NMR, and the assignment of the *syn*-structure of compound **44** was corrected by Zhao in 2014.<sup>[27]</sup> The 2,7-regioselectivity of compound **44** can be explained by the simple nucleophilic aromatic substitution ( $\text{S}_{\text{N}}\text{Ar}$ ) mechanism involving a Meisenheimer-type intermediate, which could be also confirmed by the reported reference.<sup>[28]</sup> Oxidation of **45** and **46** was readily accomplished with  $\text{PbO}_2$  to afford **47** and **48** in high yields, so as to compare the different effects between the linked and annulated heteroatoms. In contrast with the parent NDI, the absorption spectra of these heterocyclic acene diimides, especially compounds **44** and **46**, show significant redshift. Significantly, the introduction of NH bridges into acene diimides makes the resulting hydroazaacene diimides potential electron-donor materials, based on the evidence that compounds **44**, **45**, and **46** show not only two reversible reduction waves, but also reversible oxidation waves. As a matter of course, the OFET devices of compound **44** showed typical hole mobility.

In consideration that combining diimide moieties and azapentacene structures may bring about new functionalities, we also successfully synthesized a new kind of heterocyclic acene diimide, diazapentacene diimide, based on the zirconacyclopentadiene-involved cross-coupling method and dehydrogenative aromatization shown in Scheme 6.<sup>[29]</sup> The dihydrodiazapentacene diimide derivatives **50a** and **50b** were prepared by the reaction of zirconacyclopentadiene reagents **49a** and **49b** formed *in situ* from alkynes and zirconocene in dry toluene and compound **42** at  $110^\circ\text{C}$  in the presence of 2 equiv.  $\text{CuCl}$ . **50a** and **50b** were oxidized by  $\text{PbO}_2$  to afford **51a** and **51b** in high yields at room temperature. **51b**, in the same way as **29** and **30**, is an important precursor for the synthesis of higher acene diimides **52**. But all the attempts for the further aromatization of cyclohexyl of **51b** have failed. Both the NH atoms and the cyclohexyl of **50b** were resistant to further oxidation by DDQ, even at  $110^\circ\text{C}$  for five days in toluene. Compounds **50a** and **50b** have wide absorption bands and





Scheme 5. Synthesis of six-membered heterocyclic acene diimides.



Scheme 6. Synthesis of diaza-pentacene diimides.

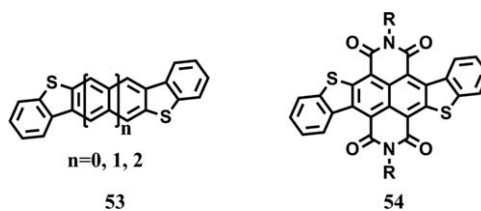


Fig. 10. Acenebisbenzothiophenes (53) and naphthobisbenzothiophene diimides (54).

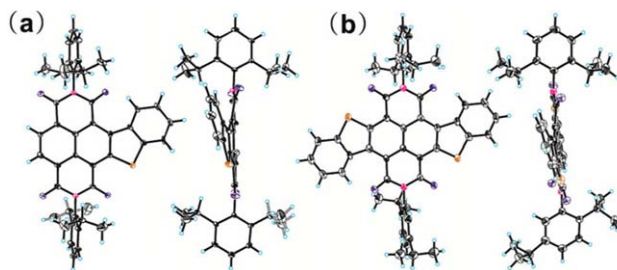
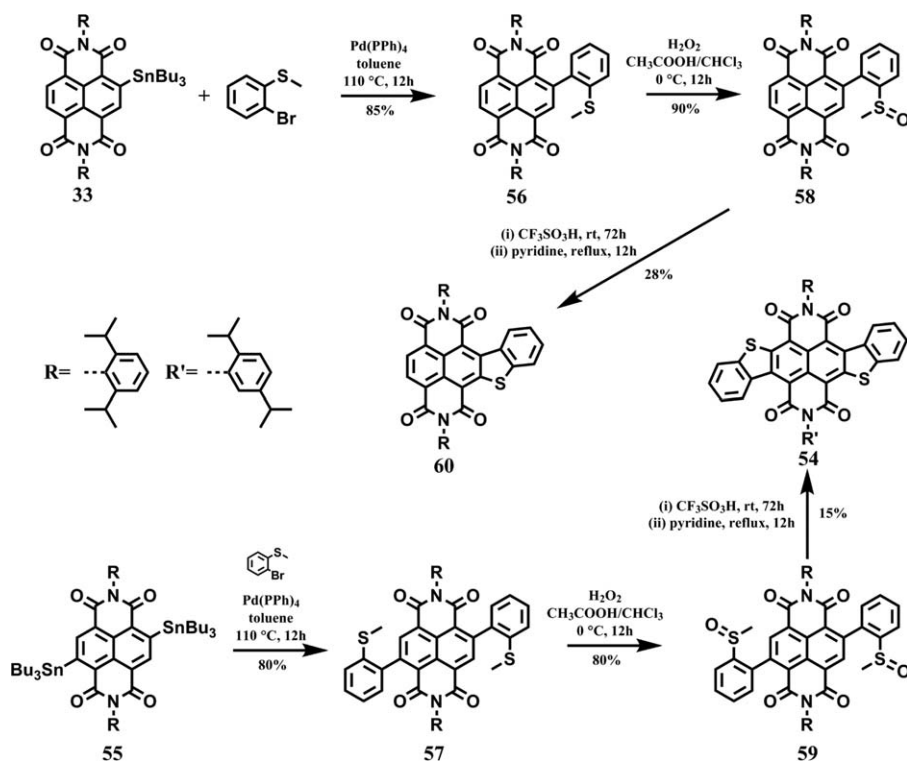


Fig. 11. X-ray crystallographic structures of: a) 60; and b) 54.

relatively high absorptivity due to two well-defined vibronic NH bridges. In contrast, 51a and 51b exhibited weaker absorptions in the whole visible and NIR region from 300 nm to 1000 nm. Comparing both with their all-carbon parents, pentacene and tetracene diimide, the absorbance maxima of



**Scheme 7.** Synthesis of naphthobisbenzothiophene diimides.

**51a** and **51b** are significantly redshifted as a reflection of the efficient  $\pi$ -conjugation and donor-acceptor interaction between the imide groups. Both **51a** and **51b** are stronger electron-accepting compounds after oxidation, with deep LUMO levels (as low as  $-4.39$  eV).

Acenebisbenzothiophenes (Figure 10, **53**) have been widely studied because of their low HOMO levels, leading to higher air stability than acenes; their close crystal packing arrangements are similar to those of acenes.<sup>[30]</sup> Specifically, benzo[1,2-*b*:4,5-*b'*]bis[*b*]benzothiophene, as an analogue of pentacene, has herringbone  $\pi$ -stacking with a plane-to-plane distance of  $3.52$  Å.<sup>[31]</sup> Moreover, OFETs based on those acenebisbenzothiophene derivatives also exhibit high charge-carrier mobilities. Therefore, we also designed and synthesized naphthobisbenzothiophene diimides (Figure 10, **54**), which are composed of a naphthobisbenzothiophene skeleton and two imide groups.<sup>[32]</sup> The synthesis process is shown in Scheme 7. Compounds **56** and **57** were prepared by Stille coupling between the key starting materials stannyl NDIs (**33** and **55**) and 2-bromothiophene in high yield in the presence of  $\text{Pd}(\text{PPh}_3)_4$ . The intermediate compounds **58** and **59**, which have poor stability, were formed by the oxidation of **56** and **57** with hydrogen peroxide in a mixture solution of glacial acetic acid and chloroform. The end products **60** and **54** were produced by the intramolecular ring closures of **58** and **59**, per-

formed with trifluoromethanesulfonic acid in the presence of phosphorus pentoxide. It is surprising that one side of the isopropyl on compound **54** was found to migrate to another position on the phenyl ring. This phenomenon, which usually occurs in the solvent of trifluoromethanesulfonic acid,<sup>[33]</sup> was further confirmed by  $^1\text{H}$  NMR and single-crystal structure (Figure 11). In light of the broad absorption, interesting packing arrangements, and strong electron-accepting abilities, these naphthobisbenzothiophene diimides are promising n-type organic semiconductors.

### 3. Properties and Applications of $\pi$ -Extended Naphthalene Diimides to Organic Semiconductors

Table 1 summarizes the optoelectronic properties and energy levels of acene diimides. The absorbance maxima of anthracene diimide **4**, tetracene diimide **28**, and pentacene diimide **6** are significantly redshifted by 99, 376, and 366 nm relative to parent NDI **3** due to the efficient  $\pi$ -conjugation and donor-acceptor interaction of the imide groups with the acene backbones. The first reduction potentials of these acene diimides are less negative than that of NDI, indicating that they are considerably stronger electron acceptors. Compounds **28** and **6** have lower LUMO levels and higher HOMO levels, leading to good ambient stabilities. Due to the asymmetrical structure of anthracene diimide **6**,

**Table 1.** Optoelectronic properties and energy levels of acene diimides.

Compds.	$\lambda_{\text{abs}}$ (nm)	$E_{\text{Ir}}^{[c]}$ (V)	$E_{\text{LUMO}}^{[d]}$ (eV)	$E_{\text{HOMO}}^{[e]}$ (eV)	$E_{\text{g}}^{[f]}$ (eV)	Ref.
<b>3</b> <sup>[a]</sup>	380	−1.03	−3.90	−7.02	3.12	[8]
<b>4</b> <sup>[b]</sup>	479	−1.02	−3.86	−6.31	2.45	[7]
<b>28</b> <sup>[a]</sup>	756	−0.80	−4.06	−5.54	1.48	[8]
<b>6</b> <sup>[b]</sup>	746	−0.68	−4.17	−5.65	1.48	[7]

[a] **3**: N,N'-di(n-octyl)-naphthalene diimide; **28**: **28a**. [b] **4**: N-iPr-ABI; **6**: N-iPr-PBI in Ref. [7]. [c] Half-wave redox potential (in V vs. Fc/Fc<sup>+</sup>). [d] Estimated from the onset potential of the first reduction wave. [e] Calculated from LUMO levels and  $E_{\text{g}}$ . [f] Obtained from the edge of the absorption spectra.

**Table 2.** Optoelectronic properties and energy levels of hybrid rylene arrays.

Compds.	$\lambda_{\text{abs}}$ (nm)	$E_{\text{Ir}}^{[a]}$ (V)	$E_{\text{LUMO}}^{[b]}$ (eV)	$E_{\text{HOMO}}^{[c]}$ (eV)	$E_{\text{g}}^{[d]}$ (eV)	Ref.
<b>38</b>	608	−0.59	−4.24	−6.10	1.86	[9a]
<b>39a</b>	610	−0.56	−4.28	−6.20	1.92	[9a]
<b>40a</b>	694	−0.51	−4.35	−6.05	1.70	[9b]

[a] Half-wave redox potential (in V vs. Fc/Fc<sup>+</sup>). [b] Estimated from the onset potential of the first reduction wave. [c] Calculated from LUMO levels and  $E_{\text{g}}$ . [d] Obtained from the edge of the absorption spectra.

**Table 3.** Optoelectronic properties and energy levels of six-membered heterocyclic acene diimides.

Compds.	$\lambda_{\text{abs}}^{[a]}$ (nm)	$\epsilon$ (M <sup>−1</sup> cm <sup>−1</sup> )	$E_{\text{LUMO}}^{[b]}$ (eV)	$E_{\text{HOMO}}^{[c]}$ (eV)	$E_{\text{g}}^{[d]}$ (eV)	Ref.
<b>43</b>	584	20,064	−3.95	−5.72	1.77	[26]
<b>44</b>	737	57,251	−3.56	−4.98	1.42	[26], [27]
<b>45</b>	618	51,747	−3.52	−5.23	1.71	[26]
<b>9</b>	796	190,000	−3.77	−5.10 <sup>[e]</sup>	1.33 <sup>[f]</sup>	[14]

[a] Measured in CHCl<sub>3</sub>. [b] Estimated from the onset potential of the first reduction wave. [c] Calculated from LUMO levels and  $E_{\text{g}}$ . [d] Obtained from the edge of the absorption spectra. [e] HOMO from CV. [f] Band gap from CV-determined LUMO and HOMO.

tetracene diimide **28** has an absorbance more redshifted to the NIR region, and a similar band gap to **6**, as a reflection of the control of the optical and electronic properties, based on the rational design of acene diimides for NIR dyes.

The optical and electronic properties and energy levels of hybrid rylene arrays based on NDI and PDI are shown in Table 2. The hybrid rylene arrays exhibit broad absorption over much of the visible region, suggesting the possible application of these arrays as active layers in organic photovoltaic cells. The low-energy maxima of **38** and **39a** are ca. 610 nm, whereas that of **40a** redshifted to 694 nm, together with higher absorptivity as a reflection of the  $\pi$ -extension along the lateral positions of rylene dyes. The energy levels of the hybrid rylene arrays from dimer to tetramer are controlled in the region of −4.2 to −4.3 eV for LUMO and −6.0 to −6.2 eV for HOMO levels, which is very exciting for the design of a large conjugated system with a smaller change in energy levels.

From Table 3, it can be seen that the six-membered heterocyclic acene diimides with the NH and S bridges also have a redshifted absorption when compared with NDI. The S-bridge-cyclized hexacene diimide **43** exhibits broad absorption in the 500 to 700 nm region with the low absorbance of 20,064 M<sup>−1</sup> cm<sup>−1</sup>. The S- and NH-bridge-cyclized hexacene diimides, **44** and **45**, have a redshifted absorption compared with **43**, together with higher absorption due to the stronger electron-donating ability of NH than S. Meanwhile, the HOMO and LUMO levels of **44** and **45** are greatly upshifted compared with NDI, which is completely opposite to that of  $\pi$ -extended acene diimides. When the NH-bridge-cyclized acene diimides expanded to the structure of hydroazaheptacene tetraimides **9**, the absorption displays a much higher absorbance of  $1.9 \times 10^5$  M<sup>−1</sup> cm<sup>−1</sup>, which provides a very useful synthetic strategy for high-performance organic solar cells.

The synthetic approaches of  $\pi$ -extended NDIs, including acene-type diimides and heterocyclic acene-type diimides and their unique optical and electronic properties, paved the way to applying these materials in OFET and OPV devices. Altogether, the lateral extension of the framework of NDIs appeared a logical next step to induce an obviously or dramatically bathochromic shift in the absorption spectrum and a narrowing of the HOMO–LUMO gap. Besides, the electronic structures and molecular packing of these  $\pi$ -extended NDIs can be flexibly controlled by the substituents introduced into the  $\pi$ -skeleton. Such a variety of  $\pi$ -extended NDIs gave us plenty of choice for their application in organic electronic devices, with LUMO energies ranging from about  $-3.9$  to  $-4.4$  eV, HOMO energies ranging from about  $-4.7$  to  $-7.0$  eV, and absorption bands covering from about 300 to 750 nm. We therefore investigated the OFET performance of the two representative compounds (**39** and **44**). Compound **39b**, as a hybrid NDI–PDI–NDI array fused with six imide groups on a huge conjugated PAH plane, is a typical n-type organic semiconductor, displaying a high thin-film electron mobility of  $0.25 \text{ cm}^2 \text{ V}^{-1} \text{ s}^{-1}$ .<sup>[9a]</sup> On the contrary, as for compound **44**, the introduction of multi-electron-donating heteroatoms to the NDI core leads to a relatively high HOMO level and turns NDIs from potential n-type materials to promising p-type semiconductors with a thin-film hole mobility of  $0.02 \text{ cm}^2 \text{ V}^{-1} \text{ s}^{-1}$ .<sup>[26]</sup> Besides thin-film OFET devices, we also took detailed investigation of the single crystalline transistors of fluoroalkyl chain substitutional NDIs. We found that the crystal has a mobility transport anisotropy along different directions.<sup>[34]</sup>

#### 4. Summary and Outlook

In this account, we summarized the recent work (since 2010) of our research group on the structures, synthetic approaches, physical and optical properties, as well as the applications of  $\pi$ -extended NDIs in organic electronic devices. Many effective synthesis strategies on core-extended naphthalene diimides have been developed. A library of more than forty acene diimides and heterocyclic acene diimide-based functional materials have been successfully synthesized and well characterized. Some preliminary results on the applications of partial molecules in OFETs indicate that the  $\pi$ -extended NDIs are promising organic semiconductors with high performance. Until now, though tetracene diimides are available, higher pure-carbon acene diimides have still been a great challenge due to synthetic difficulties. Meanwhile, the structures based on acene diimides changing from 1-dimension to 2-dimensions and 3-dimensions are very attractive to material scientists for their potential applications in OPVs. Through synthetic methodology research and structure design, we look forward to developing well-defined multidimensional acene diimides.

#### Acknowledgements

This work was financially supported by the National Natural Science Foundation of China (NSFC) (21204091, 21225209), the 973 Program (2015CB856502), and the NSFC–DFG Joint Project TRR61.

#### REFERENCES

- [1] a) W. Jiang, Y. Li, Z. H. Wang, *Chem. Soc. Rev.* **2013**, *42*, 6113–6127; b) W. Jiang, Y. Li, Z. H. Wang, *Acc. Chem. Res.* **2014**, *47*, 3135–3147.
- [2] O. D. Jurchescu, M. Popinciuc, B. J. van Wees, T. T. M. Palstra, *Adv. Mater.* **2007**, *19*, 688–692.
- [3] a) Z. Liu, G. Zhang, Z. Cai, X. Chen, H. Luo, Y. Li, J. Wang, D. Zhang, *Adv. Mater.* **2014**, *26*, 6965–6977; b) X. Zhan, A. Facchetti, S. Barlow, T. J. Marks, M. A. Ratner, M. R. Wasielewski, S. R. Marder, *Adv. Mater.* **2011**, *23*, 268–284.
- [4] a) S.-L. Suraru, F. Würthner, *Angew. Chem. Int. Ed.* **2014**, *53*, 7428–7448; b) S. V. Bhosale, C. H. Jani, S. J. Langford, *Chem. Soc. Rev.* **2008**, *37*, 331–342.
- [5] a) Z. Wang, C. Kim, A. Facchetti, T. J. Marks, *J. Am. Chem. Soc.* **2007**, *129*, 13362–13363; b) D. W. Boykin, B. Nowak-Wydra, A. L. Baumstark, *J. Heterocycl. Chem.* **1991**, *28*, 609–611; c) Y.-C. Lin, C.-H. Lin, C.-Y. Chen, S.-S. Sun, B. Pal, *Org. Biomol. Chem.* **2011**, *9*, 4507–4517; d) J. Chang, H. Qu, Z.-E. Ooi, J. Zhang, Z. Chen, J. Wu, C. Chi, *J. Mater. Chem. C* **2013**, *1*, 456–462.
- [6] A. R. Mohebbi, C. Munoz, F. Wudl, *Org. Lett.* **2011**, *13*, 2560–2563.
- [7] S. Katsuta, K. Tanaka, Y. Maruya, S. Mori, S. Masuo, T. Okujima, H. Uno, K.-i. Nakayama, H. Yamada, *Chem. Commun.* **2011**, *47*, 10112–10114.
- [8] W. Yue, J. Gao, Y. Li, W. Jiang, S. Di Motta, F. Negri, Z. Wang, *J. Am. Chem. Soc.* **2011**, *133*, 18054–18057.
- [9] a) W. Yue, A. Lv, J. Gao, W. Jiang, L. Hao, C. Li, Y. Li, L. E. Polander, S. Barlow, W. Hu, S. Di Motta, F. Negri, S. R. Marder, Z. Wang, *J. Am. Chem. Soc.* **2012**, *134*, 5770–5773; b) X. Li, C. Xiao, W. Jiang, Z. Wang, *J. Mater. Chem. C* **2013**, *1*, 7513–7518.
- [10] X. Gao, C.-a. Di, Y. Hu, X. Yang, H. Fan, F. Zhang, Y. Liu, H. Li, D. Zhu, *J. Am. Chem. Soc.* **2010**, *132*, 3697–3699.
- [11] F. Zhang, Y. Hu, T. Schuettfort, C.-a. Di, X. Gao, C. R. McNeill, L. Thomsen, S. C. B. Mannsfeld, W. Yuan, H. Sirringhaus, D. Zhu, *J. Am. Chem. Soc.* **2013**, *135*, 2338–2349.
- [12] S.-L. Suraru, U. Zschieschang, H. Klauk, F. Würthner, *Chem. Commun.* **2011**, *47*, 11504–11506.
- [13] K. Cai, Q. Yan, D. Zhao, *Chem. Sci.* **2012**, *3*, 3175–3182.
- [14] K. Cai, J. Xie, D. Zhao, *J. Am. Chem. Soc.* **2014**, *136*, 28–31.
- [15] Y. Fukutomi, M. Nakano, J.-Y. Hu, I. Osaka, K. Takimiya, *J. Am. Chem. Soc.* **2013**, *135*, 11445–11448.
- [16] F. Würthner, M. Stolte, *Chem. Commun.* **2011**, *47*, 5109–5115.



- [17] N. G. Pschirer, C. Kohl, F. Nolde, J. Qu, K. Müllen, *Angew. Chem. Int. Ed.* **2006**, *45*, 1401–1404.
- [18] a) H. Qian, F. Negri, C. Wang, Z. Wang, *J. Am. Chem. Soc.* **2008**, *130*, 17970–17976; b) H. Qian, Z. Wang, W. Yue, D. Zhu, *J. Am. Chem. Soc.* **2007**, *129*, 10664–10665; c) W. Jiang, L. Ye, X. Li, C. Xiao, F. Tan, W. Zhao, J. Hou, Z. Wang, *Chem. Commun.* **2014**, *50*, 1024–1026.
- [19] a) B. A. Jones, M. J. Ahrens, M.-H. Yoon, A. Facchetti, T. J. Marks, M. R. Wasielewski, *Angew. Chem. Int. Ed.* **2004**, *43*, 6363–6366; b) H. E. Katz, J. Johnson, A. J. Lovinger, W. Li, *J. Am. Chem. Soc.* **2000**, *122*, 7787–7792.
- [20] Y. Li, C. Li, W. Yue, W. Jiang, R. Kopecek, J. Qu, Z. Wang, *Org. Lett.* **2010**, *12*, 2374–2377.
- [21] W. Yue, Y. Zhen, Y. Li, W. Jiang, A. Lv, Z. Wang, *Org. Lett.* **2010**, *12*, 3460–3463.
- [22] Q. Ye, J. Chang, K.-W. Huang, C. Chi, *Org. Lett.* **2011**, *13*, 5960–5963.
- [23] S. Li, Z. Li, K. Nakajima, K.-i. Kanno, T. Takahashi, *Chem. Asian J.* **2009**, *4*, 294–301.
- [24] a) I. Nagao, M. Shimizu, T. Hiyama, *Angew. Chem. Int. Ed.* **2009**, *48*, 7573–7576; b) M. Shimizu, I. Nagao, Y. Tomioka, T. Hiyama, *Angew. Chem. Int. Ed.* **2008**, *47*, 8096–8099.
- [25] a) G. J. Richards, J. P. Hill, T. Mori, K. Ariga, *Org. Biomol. Chem.* **2011**, *9*, 5005–5017; b) U. H. F. Bunz, *Acc. Chem. Res.* **2015**, *48*, 1676–1686; c) Q. Miao, *Synlett* **2012**, 326–336; d) U. H. F. Bunz, *Chem. Eur. J.* **2009**, *15*, 6780–6789; e) U. H. F. Bunz, J. U. Engelhart, B. D. Lindner, M. Schaffroth, *Angew. Chem. Int. Ed.* **2013**, *52*, 3810–3821.
- [26] C. Li, C. Xiao, Y. Li, Z. Wang, *Org. Lett.* **2013**, *15*, 682–685.
- [27] K. Cai, J. Xie, X. Yang, D. Zhao, *Org. Lett.* **2014**, *16*, 1852–1855.
- [28] S.-L. Suraru, F. Würthner, *J. Org. Chem.* **2013**, *78*, 5227–5238.
- [29] C. Li, W. Jiang, X. Zhu, Z. Wang, *Asian J. Org. Chem.* **2014**, *3*, 114–117.
- [30] a) P. Gao, D. Beckmann, H. N. Tsao, X. Feng, V. Enkelmann, W. Pisula, K. Mullen, *Chem. Commun.* **2008**, 1548–1550; b) P. Gao, D. Beckmann, H. N. Tsao, X. Feng, V. Enkelmann, M. Baumgarten, W. Pisula, K. Müllen, *Adv. Mater.* **2009**, *21*, 213–216; c) Y. Zhou, W.-J. Liu, Y. Ma, H. Wang, L. Qi, Y. Cao, J. Wang, J. Pei, *J. Am. Chem. Soc.* **2007**, *129*, 12386–12387.
- [31] H. Ebata, E. Miyazaki, T. Yamamoto, K. Takimiya, *Org. Lett.* **2007**, *9*, 4499–4502.
- [32] J. Gao, Y. Li, Z. Wang, *Org. Lett.* **2013**, *15*, 1366–1369.
- [33] a) P. H. Lee, D. Kang, S. Choi, S. Kim, *Org. Lett.* **2011**, *13*, 3470–3473; b) A. Ajaz, E. C. McLaughlin, S. L. Skrabala, R. Thamatam, R. P. Johnson, *J. Org. Chem.* **2012**, *77*, 9487–9495; c) S. C. Sherman, A. V. Iretskii, M. G. White, C. Gumienny, L. M. Tolbert, D. A. Schiraldi, *J. Org. Chem.* **2002**, *67*, 2034–2041; d) G. A. Olah, O. Farooq, S. M. F. Farnia, J. A. Olah, *J. Am. Chem. Soc.* **1988**, *110*, 2560–2565; e) H. J. Bakoss, R. M. G. Roberts, A. R. Sadri, *J. Org. Chem.* **1982**, *47*, 4053–4055; f) R. M. G. Roberts, *J. Org. Chem.* **1982**, *47*, 4050–4053.
- [34] A. Lv, Y. Li, W. Yue, L. Jiang, H. Dong, G. Zhao, Q. Meng, W. Jiang, Y. He, Z. Li, Z. Wang, W. Hu, *Chem. Commun.* **2012**, *48*, 5154–5156.

---

Received: September 29, 2015

Published online: March 10, 2016